

A Butterfly Effect in Encoding-Decoding Quantum Circuits

Emanuel Dallas,^{1,*} Faidon Andreadakis,^{1,†} and Paolo Zanardi^{1,2,‡}

¹*Department of Physics and Astronomy, and Center for Quantum Information Science and Technology, University of Southern California, Los Angeles, California 90089-0484, USA*

²*Department of Mathematics, University of Southern California, Los Angeles, California 90089-2532, USA*

(Dated: September 26, 2024)

The study of information scrambling has profoundly deepened our understanding of many-body quantum systems. Much recent research has been devoted to understanding the interplay between scrambling and decoherence in open systems. Continuing in this vein, we investigate scrambling in a noisy encoding-decoding circuit model. Specifically, we consider an L -qubit circuit consisting of a Haar-random unitary, followed by noise acting on a subset of qubits, and then by the inverse unitary. Scrambling is measured using the bipartite algebraic out-of-time-order correlator (\mathcal{A} -OTOC), which allows us to track information spread between extensively sized subsystems. We derive an analytic expression for the \mathcal{A} -OTOC that depends on system size and noise strength. In the thermodynamic limit, this system displays a *butterfly effect* in which infinitesimal noise induces macroscopic information scrambling. We also perform numerical simulations while relaxing the condition of Haar-randomness, which preliminarily suggest that this effect may manifest in a larger set of circuits.

I. INTRODUCTION

The study of information spreading in quantum systems from local to non-local degrees of freedom, termed “information scrambling,” has profoundly deepened the understanding of many-body quantum systems in recent years. It has elucidated phenomena ranging from black holes [1–3] to thermalization in closed quantum systems [4] while also bolstering the underpinnings of the established field of quantum chaos [5–7]. A wide range of diagnostic tools have been employed to probe quantum chaos, such as Hamiltonian spectral statistics [8–10], the Loschmidt echo [11–13], and out-of-time-order correlators (OTOCs) [7, 14, 15]. Strongly chaotic systems may even display exponential sensitivity to small perturbations, a phenomenon familiarly known as the *butterfly effect* [16, 17].

Open system dynamics introduce an additional layer of complexity to these phenomena. Now, there is a “competition” between scrambling dynamics and information lost to decoherent noise [18]. Measurement-induced phase transitions comprise a class of such phenomena in which this competition generates complex behavior [19–21]. Recently, Lovas *et al.* have demonstrated that boundary dissipation induces a “quantum coding transition” between preserved and fully lost information in a Haar-random brickwork circuit [22]. Turkeshi and Sierant have analyzed an “encoding-decoding” circuit model in which ancillary qubits are appended to an initial multi-qubit state; all qubits are then scrambled by a random unitary, acted on by local noise, and unscrambled; then the ancillas are projected onto their initial state [23].

They observed an “error-resilience phase transition” of the fidelity between the initial and final state.

This paper, inspired by these recent results and models, investigates a similar encoding-decoding circuit model which integrates scrambling, chaos, and open system dynamics, yielding analytically tractable results. Specifically, we consider an L -qubit circuit consisting of a Haar-random unitary U , followed by identical noise processes on k qubits, followed by U^\dagger . This simple model allows us to clearly observe the effects of increasing noise strength in a state-independent manner. Of course, local Hamiltonians generate a much more restricted set of unitary dynamics than Haar random. However, random matrices provide an analytically tractable proxy for “maximally scrambling” dynamics, and the scrambling properties of locally interacting chaotic systems have been observed to quickly equilibrate to near the typical value predicted by random matrix theory [24–26].

Our metric of scrambling is the bipartite form of the algebraic out-of-time-order correlator (\mathcal{A} -OTOC [18]), introduced in [27] for closed and [5] for open systems. The bipartite \mathcal{A} -OTOC tracks the scrambling between two subsystems and has already been demonstrated as a tool for distinguishing between integrable and chaotic dynamics [5, 27]. The \mathcal{A} -OTOC, involving a Haar average over observables in each subsystem, has the nice property of depending only on the selected bipartition and dynamics, allowing us to glean very general insights. In this paper, we select for the two subsystems each half of the qubit chain to probe scrambling that is extensive in system size.

We derive an analytic formula for the \mathcal{A} -OTOC that depends on the noise channel \mathcal{E} and L . In the limit that $L \rightarrow \infty$, the formula dramatically simplifies. From this, we immediately observe a butterfly effect in which noise on finitely many qubits causes “macroscopic” scrambling. We also

* e-mail: dallas@usc.edu

† e-mail: fandread@usc.edu

‡ e-mail: zanardi@usc.edu

derive expressions for the A -OTOC under extensively scaling noise ($k \propto L$) and connect these to the competition between decoherence and scrambling. We then present multiple explicit examples and numerically demonstrate that noisy brickwork circuits accord well with theory, allowing for the possibility of observation on real quantum hardware and providing evidence that these phenomena may extend beyond Haar-random unitaries.

In section II, we provide mathematical background on the A -OTOC. In section III, we introduce the physical model we will analyze. In section IV, we present formulae for the A -OTOC under various limits and noise channels, and derive a bound on it in the $L \rightarrow \infty$ limit. In section V, we present two examples that analytically demonstrate the butterfly effect; we also numerically simulate the two examples on finitely many qubits and compare with the theory. Finally, section VI provides a summary and avenues for future work.

II. MATHEMATICAL PRELIMINARIES

A. The general A -OTOC

Let $\mathcal{H} \cong \mathbb{C}^d$ be a finite-dimensional Hilbert space representing a quantum system. Any physical observable within this system is described by a linear operator, and we denote the space of all such operators by $\mathcal{L}(\mathcal{H})$. This space, $\mathcal{L}(\mathcal{H})$, also forms a Hilbert space, equipped with the Hilbert-Schmidt inner product, defined as $\langle X, Y \rangle = \text{Tr}(X^\dagger Y)$ for operators X and Y . In the Heisenberg picture, the evolution of a physical observable $X \in \mathcal{L}(\mathcal{H})$ in an open quantum system is given by $\mathcal{E}(X)$, where \mathcal{E}^\dagger is the CPTP map governing state evolution.

The key mathematical objects in this discussion are hermitian-closed, unital subalgebras $\mathcal{A} \subset \mathcal{L}(\mathcal{H})$, which describe the degrees of freedom of interest. The commutant algebra $\mathcal{A}' = \{Y \in \mathcal{L}(\mathcal{H}) \mid [Y, X] = 0 \text{ for all } X \in \mathcal{A}\}$ captures the symmetries of \mathcal{A} and corresponds to degrees of freedom that are initially uncorrelated with \mathcal{A} . By the double commutant theorem [28], $(\mathcal{A}')' = \mathcal{A}$, so these algebras can be viewed as pairs $(\mathcal{A}, \mathcal{A}')$. During time evolution, information is exchanged between \mathcal{A} and \mathcal{A}' , which we quantify with the A -OTOC [18].

Definition 1. *The A -OTOC of algebra \mathcal{A} and channel \mathcal{E} is defined as:*

$$G_A(\mathcal{U}_t) = \frac{1}{2d} \mathbb{E}_{X_A, Y_{A'}} \left[\|X_A, \mathcal{E}(Y_{A'})\|_2^2 \right] \quad (1)$$

$\mathbb{E}_{X_A, Y_{A'}}$ denotes the Haar average over the unitaries $X_A \in \mathcal{A}$ and $Y_{A'} \in \mathcal{A}'$.

The evolution of operators in \mathcal{A}' under \mathcal{E} may lead to non-commutativity with operators in \mathcal{A} ,

which is interpreted as scrambling between the corresponding degrees of freedom.

In this paper, we reserve \mathcal{E} to refer to the map in the Heisenberg picture, and we consider maps that are CPTP in the Schrodinger picture (i.e. \mathcal{E}^\dagger is CPTP). This implies that \mathcal{E} is unital.

B. Bipartite A -OTOC

We now consider the case of bipartite algebras. Let the Hilbert space $\mathcal{H} \equiv \mathcal{H}_A \otimes \mathcal{H}_B$. Our algebra is now $\mathcal{A} = \mathbb{I}_A \otimes L(\mathcal{H}_B)$, with $\mathcal{A}' = L(\mathcal{H}_A) \otimes \mathbb{I}_B$. Henceforth, we will denote the bipartite A -OTOC as G .

In [5], the following was shown:

Proposition 1. *Let $S \equiv S_{AA'BB'}$ be the swap operator over $\mathcal{H}_{AB} \otimes \mathcal{H}_{A'B'}$. Then for a quantum channel $\mathcal{E} : \mathcal{L}(\mathcal{H}_{AB}) \rightarrow \mathcal{L}(\mathcal{H}_{AB})$, the bipartite A -OTOC is:*

$$G(\mathcal{E}) = \frac{1}{d^2} \text{Tr} \left((d_B S - S_{AA'}) \mathcal{E}^{\otimes 2}(S_{AA'}) \right). \quad (2)$$

This is the formula we use to derive our results in section IV.

An alternative formula for the A -OTOC was also derived [5]. Let us denote $\tilde{\mathcal{E}}(X) \equiv \mathcal{E}(X \otimes \frac{\mathbb{I}}{d_B})$. Then:

Proposition 2. *We denote by $\psi := |\psi\rangle\langle\psi|$ with $|\psi\rangle \in \mathcal{H}_A$. Then,*

$$G(\mathcal{E}) = N_A \mathbb{E}_\psi \left[S_L \left(\text{Tr}_B \tilde{\mathcal{E}}(\psi) \right) - d_B \left(S_L(\tilde{\mathcal{E}}(\psi)) - S_L^{\min} \right) \right] \quad (3)$$

where \mathbb{E}_ψ is the Haar average over \mathcal{H}_A , $N_A := \frac{d_A+1}{d_A}$, and $S_L^{\min} := 1 - \frac{1}{d_B}$.

We make use of this formula for numerics (section VC), in which it is easier to sample a finite set of states to reach an approximate value for $G(\mathcal{E})$. For the remainder of this paper, we will take $\mathcal{H}_A \cong (\mathbb{C}^2)^{\otimes L/2}$ to be the first set of $L/2$ qubits and $\mathcal{H}_B \cong (\mathbb{C}^2)^{\otimes L/2}$ to be the second set of $L/2$ qubits.

III. PHYSICAL SETUP

We consider a chain of L qubits, where L is even. Let U be an L -qubit unitary, and let \mathcal{E} be a single-qubit CP map. Let the adjoint action of U , in the Heisenberg picture, be denoted as \mathcal{U} , so that an operator A gets sent to $\mathcal{U}(A)$ by the action of U .

We consider the quantum map $\mathcal{C} \equiv \mathcal{U}^\dagger \mathcal{E}^{\otimes k} \mathcal{U}$ in the Heisenberg picture. For what follows, without loss of generality, we can assume that \mathcal{E} is applied to the “first” k qubit sites.

The map \mathcal{C} corresponds to a unitary evolution, a (possibly) noisy perturbation, and an undoing

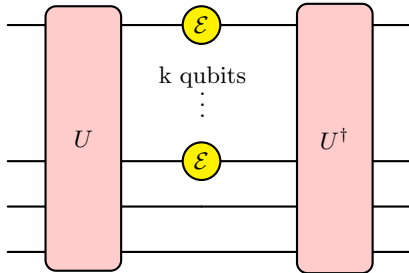


FIG. 1: Circuit diagram of \mathcal{C} .

of the unitary evolution. Analyzing the information scrambling properties of this map gives insight into the extent to which local, possibly infinitesimal perturbations can cause global, macroscopic effects – namely, this is an example of quantum chaos.

To make analytic results tractable, we calculate the average \mathcal{A} -OTOC over Haar-random U , denoted as $\overline{G(\mathcal{C})} \equiv \mathbb{E}_U G(U^\dagger \mathcal{E}^{\otimes k} U)$. For large L , the phenomenon of measure concentration implies that typical Haar-random unitaries fall close to this average [29], so it gives insight into generic behavior.

A. Connection to Loschmidt Echo

The bipartite \mathcal{A} -OTOC in this model can be viewed qualitatively as a sort of generalization of the Loschmidt echo, which we now define.

Consider a state $|\psi\rangle$ evolving under a Hamiltonian H with small perturbation V for time t . The Loschmidt echo, introduced in [11], is defined as:

$$M(t) \equiv \left| \langle \psi | e^{i(H+V)t} e^{-iHt} | \psi \rangle \right|^2. \quad (4)$$

Namely, the Loschmidt echo measures the fidelity between a state evolved by the perturbed Hamiltonian for time t and the same state evolved by the unperturbed Hamiltonian for the same time. Another, equivalent intuition is that it tracks how far $|\psi\rangle$ deviates from itself after evolving forward in time under H and backward in time under $H + V$. As such, the behavior of $M(t)$ with respect to t can reveal to what extent small perturbations yield macroscopic changes, capturing the

chaoticity of H . Its connections to scrambling and chaos have been studied extensively [12, 13].

$G(\mathcal{C})$ is an average over operators, capturing more general features of the dynamics U than a state- or operator-dependent quantity. However, like the Loschmidt echo, it captures a similar notion of evolving “forward” by U and $\mathcal{E}^{\otimes k}$ and “backward” under U^\dagger , specifically tracking the propensity of the noise to induce scrambling. Understanding the behavior of $G(\mathcal{C})$ gives insight into the chaoticity of a given U .

IV. MAIN RESULTS

To arrive at results for this model, we insert \mathcal{C} in place of the generic \mathcal{E} in proposition 1. This expression contains four copies of the unitary channel \mathcal{U} . This means that we only need unitaries drawn from a 4-design [30] to reproduce the Haar average. We can analytically compute this average by linearizing the expression and using Schur-Weyl duality [31]. The full details are presented in section VII. Since this average involves a large number of terms and group-theoretic data as inputs, we created a Mathematica notebook that performs the analytic calculations.

To simplify our results, we invoke the following:

Definition 2 (Natural representation). *Let \mathcal{E} have the Kraus representation:*

$$\mathcal{E} = \sum_i K_i(\cdot) K_i^\dagger. \quad (5)$$

*Then $X \equiv \sum_i K_i \otimes K_i^\dagger$ is the **natural representation** of \mathcal{E} .*

One can show that this representation is unique for a given map, i.e. it is independent of any particular choice of Kraus operators [32]. Since we work only with generic \mathcal{E} , we omit any subscript label on X that explicitly refers to \mathcal{E} .

This all results in the following:

Lemma IV.1 ($\overline{G(\mathcal{C})}$ for finite qubit chain). *Let \mathcal{E} be a CPTP map. Let ρ_{max} be the maximally mixed single-qubit state, γ be the purity, and S be the swap operator on $\mathcal{H}^{\otimes 2} \equiv \mathcal{H}_1 \otimes \mathcal{H}_2$. Then*

$$\overline{G(\mathcal{C})} = \left(\frac{-2^{-4k} \cdot (2^{-L} - 2^{-2L})}{(-3 + 2^L)(-2 + 2^L)(1 + 2^L)(2 + 2^L)(3 + 2^L)} \right) \cdot \left[\begin{aligned} & (2^{6L} - 2^{4L+2}) \text{Tr}(X)^{2k} - 6 \cdot 2^k (2^{4L} - 2^{2L+2}) \Re\{(\text{Tr}(\text{Tr}_1 X)^2)^k\} \\ & - 2^{2k+1} (2^{4L} - 2^{2L+1}) \text{Tr}(X)^k - 2^{k+1} (2^{4L} + 3 \cdot 2^{2L+1}) (\text{Tr}(\text{Tr}_1 X \text{Tr}_2 X))^k \\ & - 5 \cdot 2^{2k+2} 2^{2L} \Re\{(\text{Tr}(\mathcal{E} \otimes \mathbb{I}(X)))^k\} - 2^{3k+1} (2^{2L} + 6) \text{Tr}(SX^2)^k + 2^{2k} (2^{4L} - 2^{2L+2}) (\text{Tr}(X^2))^k \\ & - 2^{2k} (2^{6L} - 3 \cdot 2^{4L+2} + 22 \cdot 2^{2L}) \|X\|_2^{2k} + 2^{5k} (2^{4L} - 3 \cdot 2^{2L+2} + 12) \gamma(\mathcal{E}^\dagger(\rho_{max}))^k \end{aligned} \right]. \quad (6)$$

From this, we consider the thermodynamic limit in which $L \rightarrow \infty$. The first parenthetical term goes to $-2^{-4k} \cdot 2^{-6L}$. Thus, the only surviving terms are ones that, within the square brackets, have a prefactor of order at least 2^{6L} . We can easily see that only two terms do: $(2^{6L} - 2^{4L+2}) \text{Tr}(X)^{2k}$ and $-2^{2k} (2^{6L} - 3 \cdot 2^{4L+2} + 22 \cdot 2^{2L}) \|X\|_2^{2k}$. Keeping only their highest-ordered terms, this gives the following result.

Theorem IV.2 ($\overline{G(\mathcal{C})}$ for infinite qubit chains). *Let \mathcal{E} be a CPTP map. In the limit that $L \rightarrow \infty$, the Haar-averaged symmetric bipartite A-OTOC is given by:*

$$\overline{G(\mathcal{C})} = \left\| \frac{X}{2} \right\|_2^{2k} - \left(\frac{\text{Tr}(X)}{4} \right)^{2k}. \quad (7)$$

This is a rather striking result. In general, for an arbitrary \mathcal{E} , $\overline{G(\mathcal{C})}$ is finite, even when k is finite, i.e. $\frac{k}{L} \rightarrow 0$. An infinitesimal perturbation thereby propagates finite scrambling across an extensively scaling bipartition. One may intuitively expect such a perturbation to be vanishing in the $L \rightarrow \infty$ limit, but this is an instance of a strong butterfly effect.

We can gain intuition about this result by examining the Kraus operators of \mathcal{C} . Let $\mathcal{E}^{\otimes k}$ have the Kraus operators $\{K_i^\dagger\}_i$ in the Heisenberg picture. Since $\mathcal{E}^{\otimes k}$ is a k -qubit map, any Kraus operator K_j of $\mathcal{E}^{\otimes k}$ has support on at most k qubits. Now consider the evolution of an operator Q under the circuit \mathcal{C} . Q evolves to $\sum_i U K_i^\dagger U^\dagger Q U^\dagger K_i U$. We see that \mathcal{C} can be expressed as a CPTP map whose Kraus operators are $\{U^\dagger K_i^\dagger U\}_i$; in other words, they are the Kraus operators of $\mathcal{E}^{\otimes k}$ conjugated by U . Since U is a highly non-local, random unitary, it generally maps operators, even initially k -local ones, to other highly non-local ones. The Kraus operators of \mathcal{C} tend to have full support on all L qubits. Thus, regardless of k , so long as it is greater than zero, \mathcal{C} maps initially $L/2$ -local operators to ones with support on all L qubits.

Corollary IV.2.1 (Maximum value for extensively scaling noise). *Let $k = \alpha L$, where $\alpha \in (0, 1]$,*

and let $L \rightarrow \infty$. Then the maximum value of $\overline{G(\mathcal{C})} = 1$ is attained if and only if $\mathcal{E} = \mathcal{V}$, where V is the adjoint action of any non-identity unitary U .

Proof. By the triangle inequality,

$$\begin{aligned} \left\| \frac{X}{2} \right\|_2^{2k} &= \left\| \frac{1}{2} \sum_i K_i \otimes K_i^\dagger \right\|_2^{2k} \leq \sum_i \left\| \frac{1}{2} K_i \otimes K_i^\dagger \right\|_2^{2k} \\ &= \left(\frac{1}{2} \sum_i \|K_i\|^2 \right)^{2k} = \left(\frac{1}{2} \sum_i \text{Tr}(K_i^\dagger K_i) \right)^{2k} \\ &= \left(\frac{1}{2} \text{Tr}(\mathbb{I}) \right)^{2k} = 1, \end{aligned} \quad (8)$$

where the second-to-last equality follows from the completeness of the Kraus operators.

We know that the triangle inequality is saturated if and only if all Kraus operators are linearly dependent. Let us assume they are all proportional to some operator K , such that $K_i \equiv \alpha_i K$. In this case, $\sum_i K_i^\dagger K_i = c K^\dagger K = \mathbb{I}$, where $c = \sum_i |\alpha_i|^2$. Then $\sqrt{c} K \equiv V$ satisfies $V^\dagger V = \mathbb{I}$ and is therefore unitary. So for non-unitary maps, $(\| \frac{X}{2} \|)^{2k}$ is less than 1 and goes to 0 as $k \rightarrow \infty$. For a unitary map, $(\| \frac{X}{2} \|)^{2k}$ simply equals $(\frac{1}{2} \text{Tr}(U^\dagger U))^{2k} = 1$, saturating the inequality.

We can rewrite $\left(\frac{\text{Tr}(X)}{4} \right)^{2k}$ as $\left(\frac{1}{4} \right)^{2k} \cdot \left(\sum_i |\langle K_i, \mathbb{I} \rangle|^2 \right)^{2k}$. By the Cauchy-Schwarz inequality, we see that

$$\left(\sum_i |\langle K_i, \mathbb{I} \rangle|^2 \right)^{2k} \leq \left(\sum_i \|K_i\|^2 d \right)^{2k} = (d^2)^{2k} = 4^{2k}, \quad (9)$$

where the penultimate equality follows again from completeness of the Kraus operators. Since the Cauchy-Schwarz inequality is saturated if and only if the two operators are linearly dependent, *all* non-identity maps have $\frac{\text{Tr}(X)}{4} < \frac{4}{4} = 1$, so the second term goes to 0 as $k \rightarrow \infty$.

Thus, any non-trivial unitary satisfies $\overline{G(\mathcal{C})} = 1$ as $k \rightarrow \infty$, since the first term equals 1 and the second term goes to 0¹. Any non-unitary map has a first term that goes to 0 and a second term that goes to 0 as $k = \alpha L \rightarrow \infty$. \square

Via this proof, we have thus also proved the following:

Corollary IV.2.2 (\mathcal{A} -OTOC for extensively scaling non-unitary noise). *Let $k = \alpha L$, where $\alpha \in \{0, 1\}$, and let $L \rightarrow \infty$. Let \mathcal{E} be a non-unitary CPTP map. Then $\overline{G(\mathcal{C})} = 0$.*

We emphasize that, for open systems, $G(\mathcal{C}) = 0$ does not imply that no scrambling has occurred. Of course, if \mathcal{C} contains no noise, then the circuit in fact acts as the identity and does not scramble any information. However, $G(\mathcal{C})$ is a measure of both scrambling *and* decoherence. The other scenario in which $G(\mathcal{C}) = 0$ is when there is sufficient decoherent noise such that all of the information scrambled from A to B has dissipated out of the full system. This is the underlying reason for the result in corollary IV.2.2.

V. EXAMPLES

A. Unitary noise (Bloch sphere rotation)

Any single-qubit unitary can be represented by a rotation of the Bloch sphere by an angle θ about some axis \hat{n} . Let V be such a unitary, and let $\mathcal{E} \equiv \mathcal{V}$ act on k qubits. Then

$$\overline{G(\mathcal{C})} = 1 - \cos^{4k}(\theta). \quad (10)$$

Proof. We can represent $V \equiv e^{i\theta\hat{n}\cdot\vec{\sigma}}$. Then $X = e^{i\theta\hat{n}\cdot\vec{\sigma}} \otimes e^{-i\theta\hat{n}\cdot\vec{\sigma}}$. Since we have only one Kraus operator here, the above triangle inequality is an equality, and $\|X\|_2 = \frac{1}{2}\|V\|^2 = \frac{1}{2}\text{Tr}(V^\dagger V) = \frac{1}{2}\text{Tr}(\mathbb{I}) = 1$.

Now, for the second term, $\text{Tr}(X) = \text{Tr}(V) \cdot \text{Tr}(V^\dagger)$. We know that $e^{\pm i\theta\hat{n}\cdot\vec{\sigma}} = \cos(\theta)\mathbb{I} \pm i\sin(\theta)\hat{n}\cdot\vec{\sigma}$. Since $\hat{n}\cdot\vec{\sigma}$ is traceless, then $\text{Tr}(X) = \cos^2(\theta)\text{Tr}(\mathbb{I})^2 = 4\cos^2(\theta)$. So $\left(\frac{\text{Tr}(X)}{4}\right)^{2k} = \cos^{4k}(\theta)$, and we get the above equation. \square

The function in eq. (10) approaches 1 for increasing θ more quickly as k increases. We clearly see that the unitary corollary holds. If $k = \alpha L \rightarrow \infty$ and V is non-trivial, then the second term goes to 0 and $\overline{G(\mathcal{C})} \rightarrow 1$. Formally, for any $k \propto L$, there

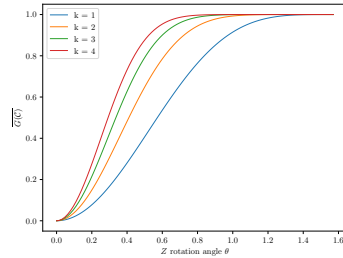


FIG. 2: $\overline{G(\mathcal{C})}$ vs. θ for small values of k . As k increases, $\overline{G(\mathcal{C})}$ approaches the step function $H(\theta)$.

is a first-order phase transition, in the thermodynamic limit, from a no-scrambling to maximally scrambled phase at $\theta = 0$.

Notice that for any (non-zero) value of k , we can achieve any value of $\overline{G(\mathcal{C})}$ by varying θ . This is a rather surprising result that warrants emphasis. By applying a $\pi/2$ rotation to a *single* qubit, we can achieve *maximal* scrambling between the two *infinitely large* halves of our bipartition, displaying a quintessential example of the butterfly effect.

B. Depolarization

Consider a channel \mathcal{E} that fully depolarizes with probability p and acts as the identity with probability $1-p$, such that, for an operator O , $\mathcal{E}(O) = p\mathbb{I} + (1-p)O$. Then \mathcal{E} have the Kraus decomposition $\left\{ \sqrt{1-\frac{3p}{4}}\mathbb{I}, \frac{\sqrt{p}}{2}\sigma^x, \frac{\sqrt{p}}{2}\sigma^y, \frac{\sqrt{p}}{2}\sigma^z \right\}$. Then

$$\overline{G(\mathcal{C})} = \left(1 - \frac{3p}{2} + \frac{3p^2}{4}\right)^k - \left(1 - \frac{3p}{4}\right)^{2k}. \quad (11)$$

Proof. It follows that

$$X = \left(1 - \frac{3p}{4}\right)\mathbb{I} \otimes \mathbb{I} + \frac{p}{4}\vec{\sigma} \cdot \vec{\sigma}. \quad (12)$$

To calculate $\|X\|^2$, we use the basic properties that the Paulis are traceless and square to identity. This gives:

$$\|X\|^2 = 4 \left(\left(1 - \frac{3p}{4}\right)^2 + 3 \left(\frac{p}{4}\right)^2 \right) = 4 - 6p + 3p^2. \quad (13)$$

And we can directly calculate:

$$\frac{\text{Tr}(X)}{4} = \frac{1}{4} \cdot 4 \cdot \left(1 - \frac{3p}{4}\right) = \left(1 - \frac{3p}{4}\right). \quad (14)$$

\square

Again, we see the second corollary follows clearly from this formula. If $p > 0$, both terms have arguments less than 1 in the exponential, and

¹ The identity map clearly gives 1 for both terms, so that the \mathcal{A} -OTOC is always 0.

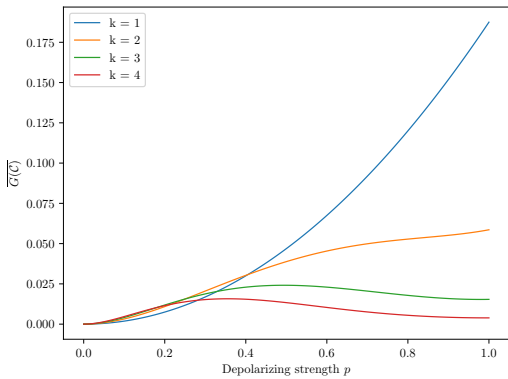


FIG. 3: $\overline{G(\mathcal{C})}$ vs. p for small values of k . As k increases, $\overline{G(\mathcal{C})}$ flattens and eventually goes to 0.

both go to 0 as $k \rightarrow \infty$. This can be understood in terms of the competition between decoherence and scrambling. The vanishing of the first term implies maximal decoherence in terms of the bipartite degrees of freedom, leading to a vanishing \mathcal{A} -OTOC. All the information that would otherwise be scrambled across the bipartition has now leaked out of the system.

With depolarization, there are no values of k for which we can achieve maximal scrambling. However, for any given finite k , $\overline{G(\mathcal{C})}$ is finite for all $p > 0$. Finite depolarization thus still produces macroscopic scrambling in infinite qubit chains. Moreover, we see that the behavior of $\overline{G(\mathcal{C})}$ with respect to p varies significantly with k . For $k = 1$ and $k = 2$, $\overline{G(\mathcal{C})}$ varies monotonically with p . For $k \geq 3$, $\overline{G(\mathcal{C})}$ is non-monotonic in p , with a peak closer to $p = 0$ as k increases. Evidently, for all $k \geq 3$, there exists a critical noise strength $p^*(k)$ above which adding more noise increases decoherence more than it increases scrambling. The parameters k and p both control the strength of decoherence and of the perturbation that leads to scrambling. Since these two effects contribute oppositely in the \mathcal{A} -OTOC, one can generally expect the existence of an optimal combination of scrambling and decoherence. Consequently, as k increases, the maximum occurs at a smaller $p^*(k)$, namely weaker perturbation and decoherence per qubit. The observation that, specifically for $k < 3$, even maximum depolarization is insufficient to produce decoherence that surpasses scrambling lacks an obvious explanation.

C. Numerics

It is natural to wonder how general the phenomena outlined in this paper are. Namely, do unitaries composed of local random “gates” display the butterfly effect? Can the Haar-randomness requirement be relaxed, and if so, what gate features correlate with the effect? We attempt to ad-

dress these questions with numerical simulations. To this end, we replace the Haar-random U with brickwork unitaries composed of $2L$ alternating layers of consecutive two-qubit gates, whose type we vary by circuit. We set $L = 8$ qubits.

We simulate three types of brickwork circuits. They are **1**) a circuit composed of Haar-random gates **2**) a circuit composed of Clifford-random gates **3**) a circuit composed of the same, repeated dual-unitary gate [33, 34]. Brickwork Haar-random circuits are known to be approximate k -designs at sufficient depth [35]. With this knowledge and the fact that this model’s \mathcal{A} -OTOC average requires a 4-design (see eq. (A5)), we know our simulated circuits are quite far from such a threshold, allowing us to observe a circuit that does not a priori approximate a Haar-random one. Similarly, Clifford circuits for qubits form a 3-design [36] while also retaining classical simulability [37]. Repeated dual-unitary brickwork circuits are useful since their entangling properties are well understood. Two-qubit dual-unitary gates are parametrized by a value that corresponds simply to their operator space entangling power [34]. Operator space entangling power is a metric of the average operator entanglement [38] generated by a unitary acting on initially unentangled, random product operators with respect to a fixed bipartition. For two-qubit gates, we take the fixed bipartition to be the “natural” one between the two qubits. By varying this parameter, we simulate dual-unitary circuits composed of varying operator space entangling power gates. Since scrambling is intimately connected with operator entanglement, studying the closeness of the dual-unitary circuits to the Haar-random result can shed insight into the extent to which operator entanglement generation is responsible for the butterfly effect in this model.

In Qiskit, it is easiest to calculate the \mathcal{A} -OTOC using proposition 2. To generate plots like the ones above, we sample 10 parameter (θ , p , respectively) values for each example. For each value, we generate 5 random brickwork circuits. Finally, for each circuit, we find $G(\mathcal{C})$ for 5 different initial $|\psi\rangle$. From these, we calculate $\overline{G(\mathcal{C})}$ for each parameter value and generate plots. Each plot also contains the $L \rightarrow \infty$ analytic curve and the $L = 8$ curve.

For unitary noise, we apply a rotation about the Z axis on a single qubit. Since our brickwork unitaries have no notion of qubit “orientation,” our results hold without loss of generality for any single-qubit unitary. We vary the rotation angle between 0 and $\frac{\pi}{2}$. For depolarizing noise, we vary p between 0 and 1 and apply the corresponding depolarization channel to a single qubit.

Both the Haar-random and Clifford-random circuits match nearly identically with the analytic formulae. Interestingly, the high (but not maximal) operator space entangling power dual-unitary

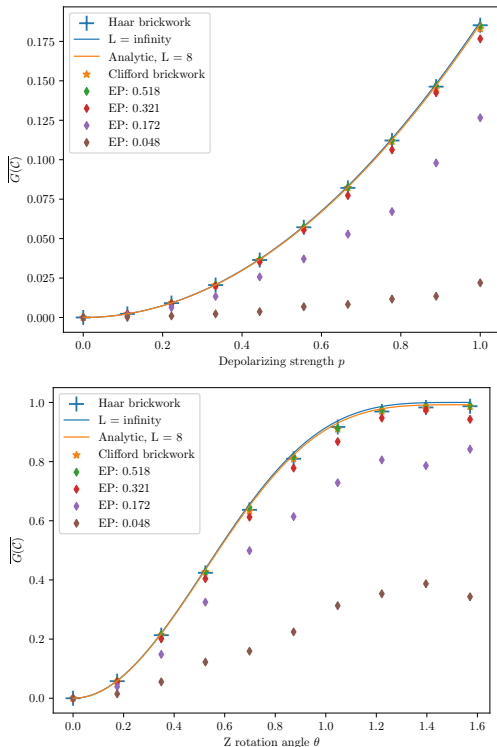


FIG. 4: Depolarizing noise strength and unitary rotation angle vs. $\overline{G(\mathcal{C})}$. The “EP” curves refer to repeated dual-unitary brickwork circuits with corresponding operator entangling power. The Haar- and Clifford-random circuits match the analytic results very closely. Increasing E_p in dual-unitary brickwork circuits increases closeness to analytic results. The standard deviations for the EP curves under unitary noise are substantial enough for θ near $\pi/2$ that the non-monotonicity cannot be deemed significant. We omit the error bars for clarity.

circuits also match nearly identically, indicating that the derived formulae may be approximated by a wider class of unitaries than just Haar-random. As the operator space entangling power of the dual-unitary gate decreases, so too does the \mathcal{A} -OTOC value. This correlates with a smaller delocalization of the perturbation from the initial qubit where it was applied, as the generation of operator entanglement decreases.

We quantify this further in fig. 5. For both noise channels, we calculate $\overline{G(\mathcal{C})} - \overline{G(\mathcal{C}_{DU})}$ at the parameter values that maximize the analytic result ($p = 1$ and $\theta = \pi/2$, respectively). This difference is plotted with respect to E_p . While a precise threshold for E_p above which the typical behavior is well approximated may be dependent on the system size and the details of the circuit, fig. 5 indicates that the operator space entangling power of the generating gate is one of the factors that contribute to the observation of the butterfly effect, even for classes of unitaries that do not form

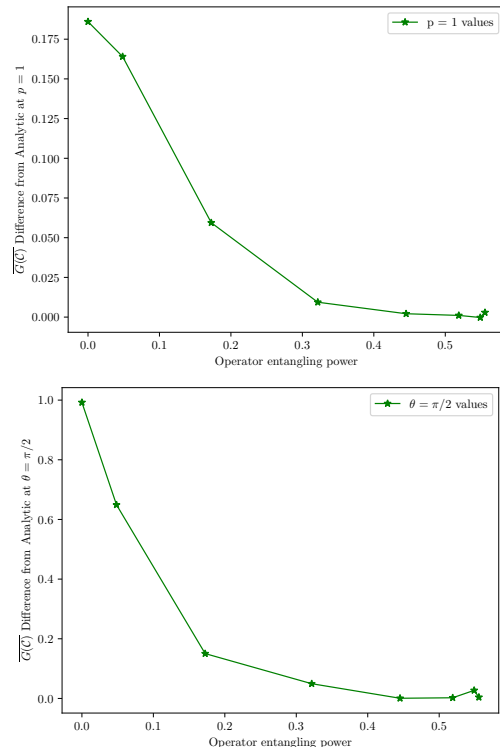


FIG. 5: Plots of deviation of dual-unitary brickworks from analytic results at argmax noise parameter values, for depolarizing and unitary noise respectively. Both curves seem to reflect a power law scaling of this difference with respect to E_p .

4-designs.

VI. CONCLUSION

We have studied a simple model circuit consisting of a Haar-random unitary U , identical noise \mathcal{E} on k qubits, and U^\dagger to explore the interconnection between scrambling, noise, and chaos. We have derived an analytic formula for the bipartite \mathcal{A} -OTOC averaged over Haar-random U , which we employ as our scrambling metric. Remarkably, our formula drastically simplifies into an elegant expression when the system size $L \rightarrow \infty$.

From this formula, it immediately becomes clear that the bipartite \mathcal{A} -OTOC, which tracks scrambling between two macroscopic subsystems, remains finite even when noise is applied only to a finite subset of qubits. This is a rather surprising instance of a butterfly effect, in which noise on as little as one qubit triggers macroscopically observable scrambling in an infinite system. We also derive formulae for the \mathcal{A} -OTOC in circuits where $k \propto L$, highlighting a fundamental distinction between dissipative and unitary noise.

To better elucidate these results, we explicitly work through the examples of depolarizing and

unitary (R_z) noise. In both cases, the \mathcal{A} -OTOC vs. noise strength curves display a strong k -dependence. For depolarizing noise, the functional shape of such curves varies sharply with k , providing another example of a butterfly-esque phenomenon – the infinite system can somehow “distinguish” between noise on one versus two qubits.

To help understand the generality of these phenomena, we have conducted numerical simulations on 8-qubit circuits for both depolarizing and unitary noise, over a range of unitary types. Haar-random and Clifford-random brickwork circuits fit very closely to the analytic Haar-random formulae. Brickwork circuits composed of highly operator space entangling dual-unitary gates closely fit the formulae as well, while those with weakly entangling dual-unitaries fall noticeably below. This preliminarily suggests that our results, and the existence of the observed butterfly effect, transcend the Haar-random unitary case. It also provides explicit evidence of the connection between gate entangling properties and circuit-wide scrambling.

The work here suggests several avenues for further theoretical development. First, the relationship between unitary type and the scrambling properties in this model is one that can be explored much further. Averages over Haar-random unitaries are convenient for their analytic tractability, but these are by no means representative of all physical processes. It would be interesting to investigate, with finite-size scaling methods, whether the numerical data we observe in our non-Haar random simulations reflect a butterfly effect in the limit $L \rightarrow \infty$. The connection between operator entangling power and the scaling of the \mathcal{A} -OTOC in this model is also worth exploring further, in the context of recent results on phase tran-

sitions in similar circuits [22, 23]; there may exist a similar threshold value above which there is a clear butterfly effect. Finally, it would be worthwhile to determine whether other information scrambling metrics display a similar effect and study their relationship to the behavior of the \mathcal{A} -OTOC.

This work also raises practical questions. The general relationship between the bipartite \mathcal{A} -OTOC and quantum channel capacity has yet to be explored. It may be interesting to explore it in this context – the modulation of noise may be able to transmit information from one end of a spin chain to another. It is also conceivable that directly measuring the \mathcal{A} -OTOC could provide information about local noise in systems where global measurements are easier to perform than local ones. Finally, it would be an experimental achievement to directly measure this circuit model on quantum hardware.

VII. ACKNOWLEDGEMENTS

ED and PZ acknowledge helpful discussions with Daniel Lidar. ED and PZ acknowledge partial support from the NSF award PHY2310227. FA acknowledges financial support from a University of Southern California “Philomela Myronis” scholarship. This research was (partially) sponsored by the Army Research Office and was accomplished under Grant Number W911NF-20-1-0075. The views and conclusions contained in this document are those of the authors and should not be interpreted as representing the official policies, either expressed or implied, of the Army Research Office or the U.S. Government. The U.S. Government is authorized to reproduce and distribute reprints for Government purposes notwithstanding any copyright notation herein.

-
- [1] Nima Lashkari, Douglas Stanford, Matthew Hastings, Tobias Osborne, and Patrick Hayden. Towards the Fast Scrambling Conjecture. *JHEP*, 04:022, 2013.
 - [2] Patrick Hayden and John Preskill. Black holes as mirrors: quantum information in random subsystems. *Journal of High Energy Physics*, 2007(09):120, sep 2007.
 - [3] Yasuhiro Sekino and Leonard Susskind. Fast Scramblers. *JHEP*, 10:065, 2008.
 - [4] Christian Gogolin and Jens Eisert. Equilibration, thermalisation, and the emergence of statistical mechanics in closed quantum systems. *Rept. Prog. Phys.*, 79(5):056001, 2016.
 - [5] Paolo Zanardi and Namit Anand. Information scrambling and chaos in open quantum systems. *Phys. Rev. A*, 103:062214, Jun 2021.
 - [6] Neil Dowling, Pavel Kos, and Kavan Modi. Scrambling Is Necessary but Not Sufficient for Chaos. *Phys. Rev. Lett.*, 131(18):180403, 2023.
 - [7] Juan Maldacena, Stephen H. Shenker, and Douglas Stanford. A bound on chaos. *JHEP*, 08:106, 2016.
 - [8] Bruno Bertini, Pavel Kos, and Toma ž Prosen. Exact spectral form factor in a minimal model of many-body quantum chaos. *Phys. Rev. Lett.*, 121:264101, Dec 2018.
 - [9] Aaron J. Friedman, Amos Chan, Andrea De Luca, and J. T. Chalker. Spectral statistics and many-body quantum chaos with conserved charge. *Phys. Rev. Lett.*, 123:210603, Nov 2019.
 - [10] Sven Gnutzmann and Uzy Smilansky. Quantum graphs: Applications to quantum chaos and universal spectral statistics. *Advances in Physics*, 55(5-6):527–625, 2006.
 - [11] Rodolfo A. Jalabert and Horacio M. Pastawski. Environment-independent decoherence rate in classically chaotic systems. *Phys. Rev. Lett.*, 86:2490–2493, Mar 2001.
 - [12] Bin Yan, Lukasz Cincio, and Wojciech H. Zurek. Information scrambling and loschmidt echo. *Phys.*

- Rev. Lett., 124:160603, Apr 2020.
- [13] Arseni Wisniacki. Loschmidt echo. *Scholarpedia*, 7(8):11687, 2012.
- [14] Daniel A. Roberts and Douglas Stanford. Diagnosing chaos using four-point functions in two-dimensional conformal field theory. *Phys. Rev. Lett.*, 115:131603, Sep 2015.
- [15] Brian Swingle. Unscrambling the physics of out-of-time-order correlators. *Nature Phys.*, 14(10):988–990, 2018.
- [16] Edward N. Lorenz. Deterministic nonperiodic flow. *Journal of Atmospheric Sciences*, 20(2):130–141, 1963.
- [17] E.N. Lorenz. *The essence of chaos*. University of Washington Press, Seattle, 1993.
- [18] Faidon Andreadakis, Namit Anand, and Paolo Zanardi. Scrambling of algebras in open quantum systems. *Phys. Rev. A*, 107:042217, Apr 2023.
- [19] Yaodong Li, Xiao Chen, and Matthew P. A. Fisher. Measurement-driven entanglement transition in hybrid quantum circuits. *Phys. Rev. B*, 100:134306, Oct 2019.
- [20] Shrabanti Dhar and Subinay Dasgupta. Measurement-induced phase transition in a quantum spin system. *Phys. Rev. A*, 93:050103, May 2016.
- [21] Brian Skinner, Jonathan Ruhman, and Adam Nahum. Measurement-induced phase transitions in the dynamics of entanglement. *Phys. Rev. X*, 9:031009, Jul 2019.
- [22] Izabella Lovas, Utkarsh Agrawal, and Sagar Vijay. Quantum coding transitions in the presence of boundary dissipation. *PRX Quantum*, 5:030327, Aug 2024.
- [23] Xhek Turkeshi and Piotr Sierant. Error-resilience phase transitions in encoding-decoding quantum circuits. *Phys. Rev. Lett.*, 132:140401, Apr 2024.
- [24] Pavel Kos, Marko Ljubotina, and Toma ž Prosen. Many-body quantum chaos: Analytic connection to random matrix theory. *Phys. Rev. X*, 8:021062, Jun 2018.
- [25] Steven W. McDonald and Allan N. Kaufman. Spectrum and eigenfunctions for a hamiltonian with stochastic trajectories. *Phys. Rev. Lett.*, 42:1189–1191, Apr 1979.
- [26] G. Casati, F. Valz-Gris, and I. Guarneri. On the connection between quantization of nonintegrable systems and statistical theory of spectra. *Lett. Nuovo Cim.*, 28(8):279–282, 1980.
- [27] Georgios Styliaris, Namit Anand, and Paolo Zanardi. Information scrambling over bipartitions: Equilibration, entropy production, and typicality. *Phys. Rev. Lett.*, 126:030601, Jan 2021.
- [28] K.R. Davidson. *C*-Algebras by Example*. Fields Institute for Research in Mathematical Sciences Toronto: Fields Institute monographs. American Mathematical Society, 1996.
- [29] M. Ledoux. *The Concentration of Measure Phenomenon*. Mathematical surveys and monographs. American Mathematical Society, 2001.
- [30] Andris Ambainis and Joseph Emerson. Quantum t-designs: t-wise independence in the quantum world. In *Twenty-Second Annual IEEE Conference on Computational Complexity (CCC'07)*, pages 129–140, 2007.
- [31] Daniel A. Roberts and Beni Yoshida. Chaos and complexity by design. *Journal of High Energy Physics (Online)*, 2017(4), 4 2017.
- [32] J. Watrous. *The Theory of Quantum Information*, pages 80–81. Cambridge University Press, 2018.
- [33] Bruno Bertini, Pavel Kos, and Toma ž Prosen. Exact correlation functions for dual-unitary lattice models in 1 + 1 dimensions. *Phys. Rev. Lett.*, 123:210601, Nov 2019.
- [34] Faidon Andreadakis, Emanuel Dallas, and Paolo Zanardi. Operator space entangling power of quantum dynamics and local operator entanglement growth in dual-unitary circuits, 2024.
- [35] Jonas Haferkamp. Random quantum circuits are approximate unitary t -designs in depth $O(nt^{5+o(1)})$. *Quantum*, 6:795, September 2022.
- [36] Zak Webb. The clifford group forms a unitary 3-design. *Quantum Inf. Comput.*, 16:1379–1400, 2015.
- [37] Daniel Gottesman. *The heisenberg representation of quantum computers*. 1998.
- [38] Paolo Zanardi. Entanglement of quantum evolutions. *Physical Review A*, 63(4):040304, March 2001.

Appendix A: Linearization of A-OTOC formula

To get the \mathcal{A} -OTOC definition 1 into a form in which we can take a Haar average over U , we rely on successive applications of the equation

$$\mathrm{Tr}(S(A \otimes B)) = \mathrm{Tr}(AB), \quad (\text{A1})$$

where S is the swap operator.

The starting point of the derivation is the proposition 1. Let $\mathcal{H}^{\otimes 4} \cong \otimes_i \mathcal{H}_i$, where each $\mathcal{H}_i \cong \mathcal{H}_{A_i} \otimes \mathcal{H}_{B_i}$. Henceforth in this section, we will take $S_{A_i A_j}$ to be the operator that swaps subsystem A_i of Hilbert space copy \mathcal{H}_i with subsystem A_j of Hilbert space copy \mathcal{H}_j . We will take S_{ij} to be the swap between \mathcal{H}_i and \mathcal{H}_j .

To improve readability, let $d_B S_{ij} - S_{A_i A_j} \equiv M_{ij}$ (see proposition 1), and let the Kraus operators of $\mathcal{E}^{\otimes 2}$ be $\{\Lambda_\alpha\}_\alpha$.

Rewriting proposition 1, we have

$$G(\mathcal{C}) = \frac{1}{d^2} \mathrm{Tr}(M_{12}(\mathcal{U}^\dagger)^{\otimes 2} \mathcal{E}^{\otimes 2} \mathcal{U}^{\otimes 2}(S_{A_1 A_2})). \quad (\text{A2})$$

Expanding this gives

$$G(\mathcal{C}) = \frac{1}{d^2} \sum_{\alpha} \text{Tr}((U^\dagger)^{\otimes 2} \Lambda_{\alpha} U^{\otimes 2} S_{A_1 A_2} (U^\dagger)^{\otimes 2} \Lambda_{\alpha}^\dagger U^{\otimes 2} M_{12}). \quad (\text{A3})$$

Now we use the swap identity and expand from $\mathcal{H}^{\otimes 2}$ to $\mathcal{H}^{\otimes 4}$:

$$= \frac{1}{d^2} \sum_{\alpha} \text{Tr}(S_{13} S_{24} (U^\dagger)^{\otimes 4} (\Lambda_{\alpha} \otimes \Lambda_{\alpha}^\dagger) (U^{\otimes 4}) (S_{A_1 A_2} \otimes M_{34})). \quad (\text{A4})$$

Finally, expanding out M_{34} , we get:

$$G(\mathcal{C}) = \frac{1}{d^2} \text{Tr} \left(S_{13} S_{24} (U^\dagger)^{\otimes 4} \left(\sum_{\alpha} \Lambda_{\alpha} \otimes \Lambda_{\alpha}^\dagger \right) U^{\otimes 4} (S_{A_1 A_2} \otimes (d_B S_{34} - S_{A_3 A_4})) \right). \quad (\text{A5})$$

Now, to calculate $\overline{G(\mathcal{C})}$, we must to evaluate the following (and plug back into the above formula):

$$\mathbb{E}_{U \in \mathcal{U}(2^L)} \left[(U^\dagger)^{\otimes 4} \left(\sum_{\alpha} \Lambda_{\alpha} \otimes \Lambda_{\alpha}^\dagger \right) U^{\otimes 4} \right].$$

Note that the set of Kraus operators $\{\Lambda_{\alpha}\}_{\alpha}$ of $\mathcal{E}^{\otimes 2}$ is just the set of all tensor products of Kraus operators of \mathcal{E} , namely $\{K_i\}_i$. Thus,

$$\sum_{\alpha} \Lambda_{\alpha} \otimes \Lambda_{\alpha}^\dagger = \sum_{ij} K_i \otimes K_j \otimes K_i^\dagger \otimes K_j^\dagger. \quad (\text{A6})$$

This operator will take the place of O in what follows for the final calculation.

Appendix B: Schur-Weyl Duality

Here, we follow the articulate notation of the supplementary material of [23]. To simplify the subsequent equations, let

$$\Phi_{\text{Haar}}^{(k)}(O) = \mathbb{E}_{U \in \mathcal{U}(2^L)} \left[(U^\dagger)^{\otimes k} O U^{\otimes k} \right] \equiv \int_{\text{Haar}} d\mu(U) (U^\dagger)^{\otimes k} O U^{\otimes k}. \quad (\text{B1})$$

Via Schur-Weyl duality [31], it follows that:

$$\Phi_{\text{Haar}}^{(k)}(O) = \sum_{\pi \in \mathcal{S}_k} b_{\pi}(O) T_{\pi}, \quad (\text{B2})$$

where \mathcal{S}_k is the permutation group over k elements and T_{π} is the representation of the permutation π acting on $(\mathbb{C}^{2^L})^{\otimes k}$. Note that $T_{\pi} = \otimes_{i=1}^k t_{\pi}^{(i)}$, where $t_{\pi}^{(i)}$ is the representation of π on the i -th qubit, i.e. each of these permutations is the tensor of single-qubit permutations across the k copies of the system Hilbert space.

It further follows that:

$$b_{\pi} = \sum_{\sigma \in \mathcal{S}_k} W_{\pi, \sigma} \text{Tr}(O T_{\sigma}), \quad (\text{B3})$$

where $W_{\pi, \sigma}$ is the *Weingarten symbol* corresponding to the permutations π, σ .

Recall that for the symmetric group \mathcal{S}_k , the irreps correspond to the integer partitions of k . An integer partition of k is an (ordered, for uniqueness) set of positive integers which add up to k . Let λ refer to an arbitrary integer partition of k , let Π_{λ} be the projection onto the irrep (corresponding to) λ , d_{λ} be the irrep's dimension, and χ_{λ} be its character function. Then

$$W_{\pi, \sigma} = \sum_{\lambda \vdash k} \frac{d_{\lambda}^2}{(k!)^2} \frac{\chi_{\lambda}(\pi\sigma)}{\text{tr}(\Pi_{\lambda})}. \quad (\text{B4})$$

To calculate the traces in eq. (B3), we make use of the following identity. Let $T_\sigma \in \mathcal{S}_4$ have the cyclic representation $(ab)(cd)$, where $\{a\dots d\} \in \{1, 2, 3, 4\}$ ². Let $O = \otimes_{k=1}^4 M_k$. Then

$$\text{Tr}(T_\sigma O) = \text{Tr}(M_a M_b) \text{Tr}(M_c M_d). \quad (\text{B5})$$

This is just a simple generalization of the above swap formula.

Finally, to yield the formulae in section IV, we created a Mathematica notebook, making use of the excellent group-theoretic functions written in the notebook of [23].

² The choice of a (2, 2) cycle structure here is arbitrary and made to illustrate the identity.